ARTICLES

Journal of Semiconductors
(2021) 42, 122803
doi: 10.1088/1674-4926/42/12/122803

Low-threshold lasing in a plasmonic laser using nanoplate InGaN/GaN

Ting Zhi[1, 2], Tao Tao[3, 4, †], Xiaoyan Liu[1, 2], Junjun Xue[1, 2], Jin Wang[1, 2], Zhikuo Tao[1, 2], Yi Li[5, 6], Zili Xie[3, 4], and Bin Liu[3, 4]

[1]College of Electronic and Optical Engineering, Nanjing University of Posts and Telecommunications, Nanjing 210023, China

[2]College of Microelectronics, Nanjing University of Posts and Telecommunications, Nanjing 210023, China

[3]Jiangsu Provincial Key Laboratory of Advanced Photonic and Electronic Materials, School of Electronic Science and Engineering, Nanjing University, Nanjing 210093, China

[4]Nanjing National Laboratory of Microstructures, Nanjing University, Nanjing 210093, China

[5]School of Information Science and Technology, Nantong University, Nantong 226019, China

[6]Tongke School of Microelectronics, Nantong University, Nantong 226019, China

Abstract: Plasmonic nanolaser as a new type of ultra-small laser, has gain wide interests due to its breaking diffraction limit of light and fast carrier dynamics characters. Normally, the main problem that need to be solved for plasmonic nanolaser is high loss induced by optical and ohmic losses, which leads to the low quality factor. In this work, InGaN/GaN nanoplate plasmonic nanolaser with large interface area were designed and fabricated, where the overlap between SPs and excitons can be enhanced. The lasing threshold is calculated to be ~6.36 kW/cm^2, where the full width at half maximum (FWHM) drops from 27 to 4 nm. And the fast decay time at 502 nm (sharp peak of stimulated lasing) is estimated to be 0.42 ns. Enhanced lasing characters are mainly attributed to the strong confinement of electromagnetic wave in the low refractive index material, which improve the near field coupling between SPs and excitons. Such plasmonic laser should be useful in data storage applications, biological application, light communication, especially for optoelectronic devices integrated into a system on a chip.

Key words: surface plasmon; plasmonic laser; GaN

Citation: T Zhi, T Tao, X Y Liu, J J Xue, J Wang, Z K Tao, Y Li, Z L Xie, and B Liu, Low-threshold lasing in a plasmonic laser using nanoplate InGaN/GaN[J]. *J. Semicond.*, 2021, 42(12), 122803. http://doi.org/10.1088/1674-4926/42/12/122803

1. Introduction

Due to small physic scale and low power dissipation, miniaturized lasers are important for high resolution displays[1], ultrafast optical communication[2], sophisticated biomedical imaging[3] and on-chip integration with IC design application[4]. In the past two decades, tremendous efforts based on metal-coated photonic cavity[5], Fabry–Pérot (F–P) cavity[6], whispering-gallery[7] and ring cavity[8] have been achieved. However, optical cavity is fundamental in laser design, whose physic size has faced a bottleneck because of the diffraction limit of light ($\lambda/2n$, where λ is wavelength, n is refractive index of dielectric medium)[9]. One new type of sub-wavelength nanolaser was proposed by Prof. Zhang in 2009, based on the principle of the surface plasmon amplification of stimulated emission of radiation (SPASER), which demonstrates the ability to break the diffraction limit of light[10]. In the plasmonic laser, surface plasmon polaritons (SPPs) act an important role, collected electronic oscillations of dielectric and metal interface, which gives promise for a light source capable of reconciling photonic and electronic length scales. Ma *et al.* demonstrated a hybrid SPASER consisting of cadmium sulfide (CdS) nanowires separated from a silver film by nanoscale magnesium fluoride (MgF_2) at room temperature[11]. Recent efforts in plasmonic laser were focusd on reducing the intrinsic ohmic who is mainly determined by the metal itself[12, 13]. However, the extrinsic loss, determined by plasmonic cavity (facet reflectance, interface area, and symmetry), is also a major challenge in efficiency and threshold of plasmonic laser.

In the work, plasmonic nanolaser based on nanoplate InGaN/GaN was designed via increasing interface area and symmetry at room temperature, which consisted of gain material (nanoplate InGaN/GaN), low refractive index medium (thin SiO_2 film) and noble metal film (Silver layer). The threshold is calculated to be ~6.36 kW/cm^2, where the FWHM drops from 27 to 4 nm. Moreover, the fast decay time at 502 nm (sharp peak of stimulated lasing) is estimated to be 0.42 ns, indicating a much faster radiative channel. The design plasmonic laser using nano-plate of gain material relatively decreases the edge-scattering ratio, enhances overlap of SPs and excitons, and further holds strong confinement of electromagnetic wave in the low refractive index material.

2. Experimental section

2.1. Growth of gain material

The gain material (GaN/InGaN) was grown on sapphire (0002) substrate by metal-organic chemical vapour deposition (MOCVD). N_2 and H_2 act as carrier gases for the growth of InGaN and GaN epitaxial layers. After growth, the gain ma-

Correspondence to: T Tao, ttao@nju.edu.cn
Received 2 SEPTEMBER 2021; Revised 30 SEPTEMBER 2021.

terial consisted of a 2 μm undoped GaN buffer layer, a 2 μm silicon-doped n-type GaN layer, 15 periods ($In_xGa_{1-x}N$: 3.5 nm/GaN: 12 nm) of multiple quantum wells (MQWs), a 25 nm $Al_{0.25}Ga_{0.75}N$ layer as an electron-blocking layer, and a 500 nm-thick Mg-doped p-type GaN layer. The In composition (x) was set to be 0.35 in the MQWs region for green emission.

2.2. Fabrication of nano-plate

First of all, the gain material was cleaned with acetone, methanol and then deionized water. In order to form nano-plate, custom-made nano-mask and following inductively coupled plasma (ICP) etching process are necessary. Thus, a thick SiO_2 layer (~300 nm) was deposited on the gain material sample as the hard mask, where plasma-enhanced chemical vapour deposition (PECVD) was applied at 300 °C. Subsequently, a thin PMMA layer was spin-coated and patterned by electron beam lithography (EBL). The width and length of nano-sized pattern were set as 0.2 and 1 μm, respectively. The pattern on PMMA layer were reversed in order to acquiring nano-sized metal mask after lift-off process. Therefore, 20 nm-thick nickel were deposited by physical vapor deposition (PVD 75, Kurt J. Lesker) on PMMA layer and lifted-off by warm 1-methyl-2-pyrrolidinone. One more reactive-ion etching (RIE) process was carried out to transform nickel pattern into SiO_2 layer as a second reinforced mask. Finally, the gain material with nickel and SiO_2 patterned masks was etched using ICP system, where the height of gain material can be controlled to be 3 μm. A set of chemical treatments were carried out: the hot (80 °C) potassium hydroxide for 8 min and following the nitric acid for 2 min, which effectively minimized the surface roughness and defects caused by the ICP etching.

2.3. Preparation of substrate

A undoped silicon substrate was prepared by cleaning with acetone, methanol and then deionized water. A 300 nm SiO_2 layer was deposited by PECVD as an insulation material. It has been widely reported that smooth metal surface could dramatically reduce losses, including ohmic and scattering losses[14]. Therefore, a silver film (~30 nm) was deposited on SiO_2 layer at a slow speed (0.1 Å/s) by PVD. During the deposition process, the sample was maintained under a constant temperature of 25 °C and at a rapid rotation rate of 20 rpm to get a uniform thickness over a large area. It should be mentioned that the following thin SiO_2 layer need to be carefully optimized. In this work, the growth conditions for high-quality thin SiO_2 layer were set as: the silicane/nitric oxide (SiH_4/N_2O) ratio was approximately 100/450, the RF power was set to be 10 W, and the reactor pressure was maintained at 300 mTorr. After deposited, the thin SiO_2 gap is about 10 nm.

2.4. Characterization of SPASER

The surface morphology of the samples was measured using a JEOL JSM 7000F field emission scanning electron microscopy (SEM). The photoluminescence (PL) spectra were collected by confocal microscopy equipped with a 40× UV objective lens (Mitutoyo, numerical aperture = 0.5). The lasing beam was focused on a 5 μm-diameter spot coving the whole nano samples at an incident angle of 90°. For fluorescence lifetime measurements, a commercial time-resolved photoluminescence (TRPL) system with time-correlated single photon counting (TCSPC) module was applied, where a 375 nm picosecond laser with pulse width of ~40 ps was used as the excitation source. The parameters for TRPL system were calibrated before for the measurements of all samples.

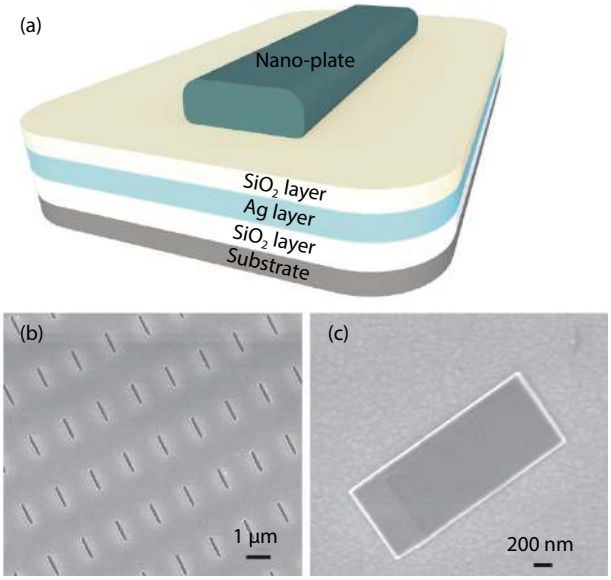

Fig. 1. (Color online) (a) Schematic of the nano-plate based SPASER sample, where a thin nano-plate atop silver layer separated by a 10 nm SiO_2 gap. (b) SEM image of nano-plate arrays. (c) SEM image of SPASER with single nano-plate (200 nm in width, 1 μm in length, 3μm in height).

3. Results and discussion

Fig. 1(a) shows the schematic structure of the SPASER, which consists of GaN/InGaN nano-plate, ultra-thin SiO_2 layer, the Ag film, SiO_2 insulation layer and Si substrate. After EBL and ICP etching process, The SEM image in Fig. 1(b) displays the nano-plate arrays of gain material with a configuration of 200 nm in width, 1 μm in length and 3 μm in height. After mechanical cut and transfer nano-plate onto the prepared Si substrate, nano-plate based SPASER samples are prepared as illustrated by the SEM image in Fig. 1(c). It has been widely reported that rough surface and defects on the sidewall of gain material will cause scattering loss and optical leakage, which limits the corresponding gain from SPs[15–17]. Hence, the fabrication of nano-plate gain material was optimized to acquire smooth and vertical sidewalls as illustrated in Fig. 1(c), where the most intense electric fields can be confined in the SPASER.

The photoluminescence (PL) spectra of single nano-plate without Ag film were measured by increasing the optical pumping power density using a micro-PL system excited by a continuous 405-nm laser. A typical spontaneous emission of InGaN/GaN nano-plate can be seen in Fig. 2(a). As the optical pumping power density increasing from 1.27 to 19.11 kW/cm^2, the emission peak shifts to 501 nm, indicating a typical spontaneous emission behavior due to the band filling effect and carrier screen in InGaN/GaN gain material[18]. The FWHM of the PL spectra oscillates between 26 and 28 nm, as shown by the black square line curve in Fig. 2(b). No "S" shape can be identified (blue square line curve) in the light–light (L–L) plot, which is similar to the results in our previous reports[19, 20].

On the other hand, sharp peaks appear at 502 nm for

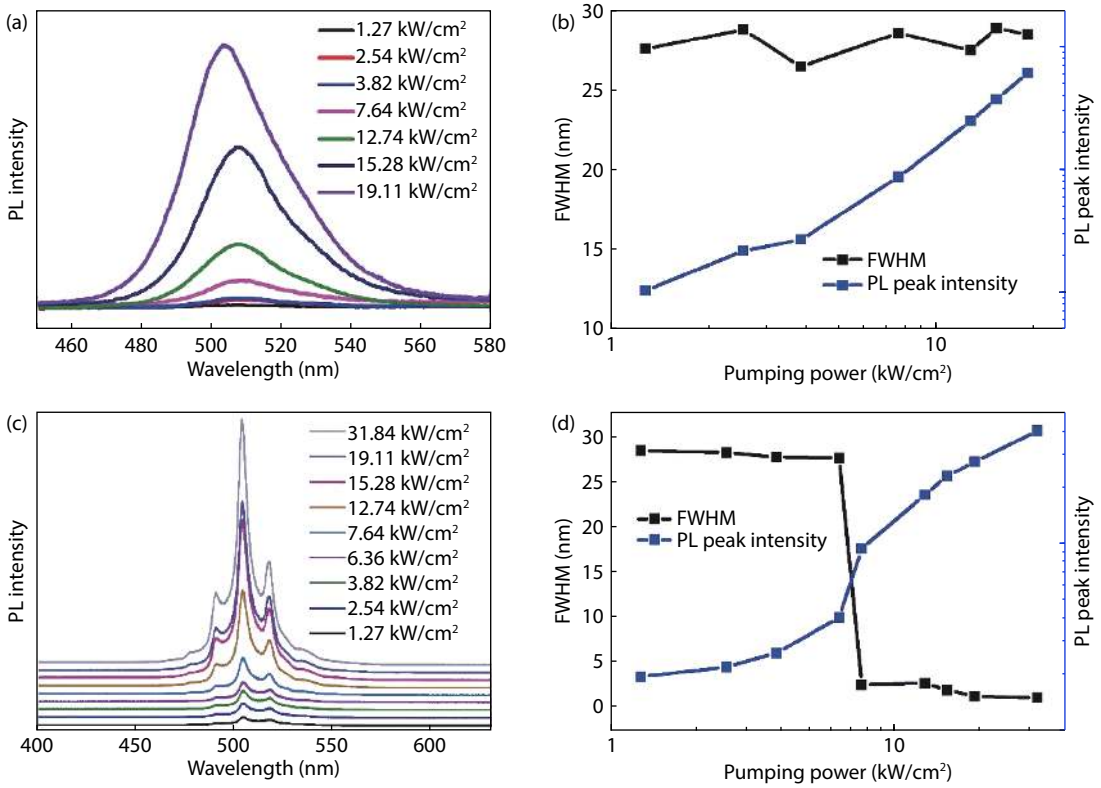

Fig. 2. (Color online) (a) The PL spectra of nano-plate without Ag film under different optical pumping power density. (b) Corresponding L–L curve of the PL peak intensity and the FWHM in the log–log scale as a function of optical pumping power density. (c) PL emission of SPASER with increasing the same optical pumping power density. (d) Corresponding L–L curve and FWHM of the dominant lasing peak at 502 nm as a function of the excited power density.

SPASER samples under a very low pumping power density, as shown in Fig. 2(c). A small peak shift from 510 to 502 nm with respect to the increasing pumping power reveal a reduced frequency pulling effect due to the strong coupling between SPs and excitons. In Fig. 2(d), an obvious nonlinear "S" shape can be seen, where the lasing threshold can be roughly estimated to be 6.36 kW/cm^2. Near the lasing threshold, the FWHM drops from 27 to 4 nm, further confirming the transition from spontaneous emission to stimulated emission. And the quality factor[19], determined by $Q = \lambda/\Delta\lambda$, where λ and $\Delta\lambda$ are the central emission wavelength and FWHM, is about 130 under the optical pumping power of 19.11 kW/cm^2. The PL spectra of current SPASER exhibit multiple lasing peaks, which is attributed to a number of available modes in the nano-plate cavity configuration. The β factor of laser can be calculated by the ratio of output light intensity below and above the threshold[19]. In this work, the β factor is 0.125, indicating a high ratio of lasing mode where spontaneous recombination is suppressed.

The simulated electric field of nano-plate based SPASER samples with/without Ag film was obtained via finite-difference time-domain calculations (FDTD Solutions from Lumerical Solutions). In the simulation, a dipole source was used as a light source with a wide spectral range from 200 to 600 nm. The Ag parameter was adopted from the dielectric function of Palik, and the refraction index of the SiO_2 was measured to be 1.46 by an ellipsometer. As illustrated by the simulated cross-sectional electric field distribution in Fig. 3(a), the electromagnetic field can be highly confined within the low-permittivity SiO_2 layer with an ultra-small volume in SPASER structure. In another word, the electromagnetic field was confined into an extremely thin waveguide, which is as much as 10 times smaller than the diffraction-limited spot. It should be mentioned that the nano-plate SPASER designed in this work, compared to the cylinder structure in our previous reports[19, 20], are helpful for improving the surface plasma coupling between gain material and surface plasma metal. In contrast, the simulated cross-sectional electric distribute of nano-plate without Ag indicates low confinement of electric field and relatively large mode volume as shown in Fig. 3(b). It suggests that the spontaneous emission might still be dominant under the same optical pumping density. Meanwhile, the effective and group effective indices of SPASER samples were simulated by the eigenmode method (MODE solutions from Lumerical Solutions). The group index (n_g, the ratio of the vacuum velocity of light to the group velocity of the cavity mode) can be determined by the relationship[17] $n_g(\lambda) = n_{eff}(\lambda) - \lambda[dn_{eff}(\lambda)/d\lambda]$, where λ is the emission wavelength, and $n_{eff}(\lambda)$ is the effective index. The value of the group index in SPASER and nano-plate structures is 7 at 502 nm and 2 at 520 nm, respectively, suggesting an effectively enhanced modal gain in the SPASER structure.

To further understand the mechanism of exciton recombination in SPASER, μ-TRPL of the nano-plate and SPASER were preformed at room temperature and shown in Fig. 4. A standard 2-exponential component model was calculated to study the carrier dynamics for emission. The TRPL traces can be described by[20, 21],

$$I(t) \approx A_1 \exp(-t/\tau_0) + A_2 \exp(-t/\tau_1),$$

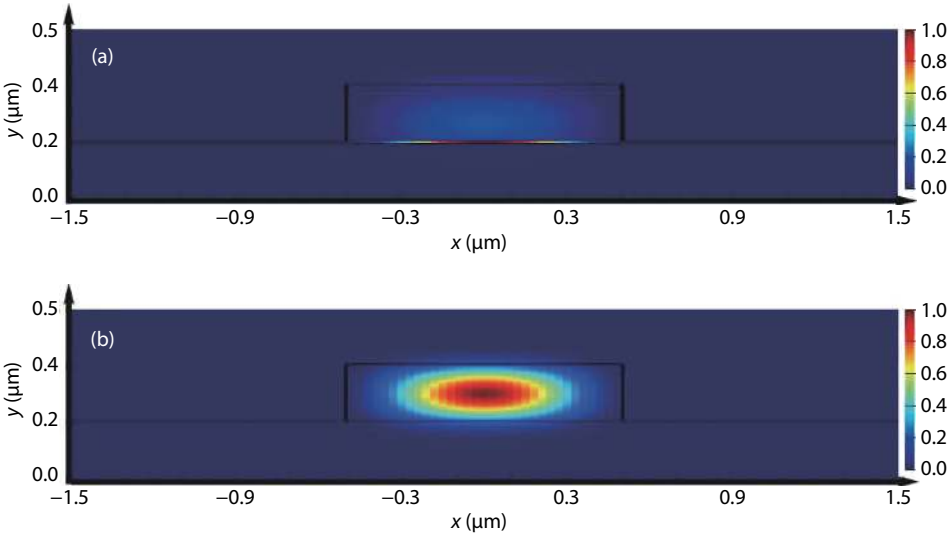

Fig. 3. (Color online) (a) Simulated electric field distribution of plasmonic laser at 502 nm. (b) Simulated electric field distribution of the Nano-plate gain material without Ag film at 520 nm.

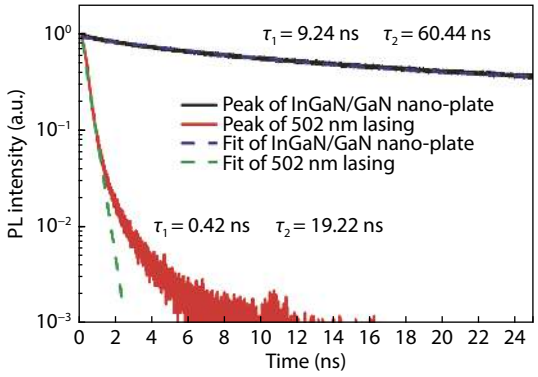

Fig. 4. (Color online) TRPL spectra of SPASER at the peak of 502 nm (red line) and InGaN/GaN nano-plate at the peak of 520 nm (black line).

where A_1 and τ_0 (A_2 and τ_1) are the fast (slow) decay components. In typical InGaN/GaN gain materials, the intrinsic lifetime is dominated by the intrinsic radiative (τ_r) and non-radiative (τ_{nr}) decay times ($1/\tau_0 = 1/\tau_{nr} + 1/\tau_r$) at room temperature[22]. For the Nano-plate gain material, the fast decay time τ_0 at 520 nm (dominate peak of spontaneous emssison) is estimated to be 9.24 ns, similar to the intrinsic lifetime of ordinary InGaN emission. However, for the SPASER, the fast decay time τ_0 at 502 nm (sharp peak of stimulated lasing) is estimated to be 0.42 ns, indicating a much faster radiative channel. In the plasmonic laser, the energy is transferred from excitons to SPP. Four steps are proposed: 1) many pairs of electrons and holes are excited in the gain material by optical pumping; 2) surface plasmon remain stable in SPASER structure via excitation of suitable light pumping; 3) energy is transferred between surface plasmon metal system and stimulated excitons to create more excitons and surface plasmons; 4) decoupling occurs at the boundary of gain material and emit lasing. In this work, nano-plate gain material was designed to decrease the edge-scattering ratio and significantly enhance the overlap between SPs and excitons compared to the plasmonic lasers using cylinder structure. Strong confinement of electromagnetic wave in the low refractive index material support for the high gain in nano-plate SPASER samples. Such nano-plate design should be useful in light communication, data storage applications, biological application, especially for optoelectronic devices integrated into a system on a chip.

4. Conclusion

In summary, new plasmonic laser was designed and demonstrated at visible wavelength based on the nano-plate SPASER structure, consisting of gain material (InGaN/GaN nano-plate), low refractive index medium (thin SiO_2 film) and noble metal film (silver layer). The designed nano-plate gain material holds strong confinement of electromagnetic wave in the low refractive index material, where larger interface area enhances the overlap of SPs and excitons and decrease the edge-scattering ratio. As a result, the room temperature lasing threshold is reduced to be ~6.36 kW/cm^2, where the FWHM drops from 27 to 4 nm. The present work paves the way for light communication, data storage applications, biological application, especially for optoelectronic devices integrated into a system on a chip.

Acknowledgements

The authors acknowledge financial support from the National Natural Science Foundation of China (62004104, 61974062, 61921005), the Nature Science Foundation of Jiangsu Province (BK20180747 and BE2015111), the Solid State Lighting and Energy-saving Electronics Collaborative Innovation Center, and Research Funds from NJU-Yangzhou Institute of Opto-electronics.

References

[1] Goh X M, Zheng Y H, Tan S J, et al. Three-dimensional plasmonic stereoscopic prints in full colour. Nat Commun, 2014, 5, 1
[2] Murphy E. Enabling optical communication. Nature Photon, 2010, 4, 287
[3] Chen Y C, Chen Q S, Fan X D. Lasing in blood. Optica, 2016, 3, 809
[4] Tchernycheva M, Messanvi A, de Luna Bugallo A, et al. Integrated photonic platform based on InGaN/GaN nanowire emitters and detectors. Nano Lett, 2014, 14, 3515

[5] Hill M T, Oei Y S, Smalbrugge B, et al. Lasing in metallic-coated nanocavities. Nat Photonics, 2007, 1, 589
[6] Chang S W, Lin T R, Chuang S L. Theory of plasmonic fabry-perot nanolasers. Opt Express, 2010, 18, 15039
[7] McCall S L, Levi A F J, Slusher R E, et al. Whispering-gallery mode microdisk lasers. Appl Phys Lett, 1992, 60, 289
[8] Ma R M, Wei X L, Dai L, et al. Light coupling and modulation in coupled nanowire ring-Fabry-Pérot cavity. Nano Lett, 2009, 9, 2697
[9] Bergman D J, Stockman M I. Surface plasmon amplification by stimulated emission of radiation: Quantum generation of coherent surface plasmons in nanosystems. Phys Rev Lett, 2003, 90, 027402
[10] Oulton R F, Sorger V J, Zentgraf T, et al. Plasmon lasers at deep subwavelength scale. Nature, 2009, 461, 629
[11] Ma R M, Oulton R F, Sorger V J, et al. Room-temperature sub-diffraction-limited plasmon laser by total internal reflection. Nat Mater, 2011, 10, 110
[12] Lu Y J, Wang C Y, Kim J, et al. All-color plasmonic nanolasers with ultralow thresholds: Autotuning mechanism for single-mode lasing. Nano Lett, 2014, 14, 4381
[13] González-Tudela A, Huidobro P A, Martín-Moreno L, et al. Theory of strong coupling between quantum emitters and propagating surface plasmons. Phys Rev Lett, 2013, 110, 126801
[14] Eaton S W, Fu A, Wong A B, et al. Semiconductor nanowire lasers. Nat Rev Mater, 2016, 1, 1
[15] Liu S L, Sheng B W, Wang X Q, et al. Molecular beam epitaxy of single-crystalline aluminum film for low threshold ultraviolet plasmonic nanolasers. Appl Phys Lett, 2018, 112, 231904
[16] Ma Y G, Guo X, Wu X Q, et al. Semiconductor nanowire lasers. Adv Opt Photon, 2013, 5, 216
[17] Zhang Q, Li G, Liu X, et al. A room temperature low-threshold ultraviolet plasmonic nanolaser. Nat Commun, 2014, 5, 4953
[18] Tian P F, McKendry J J D, Gu E D, et al. Fabrication, characterization and applications of flexible vertical InGaN micro-light emitting diode arrays. Opt Express, 2016, 24, 699
[19] Tao T, Zhi T, Liu B, et al. Manipulable and hybridized, ultralow-threshold lasing in a plasmonic laser using elliptical InGaN/GaN nanorods. Adv Funct Mater, 2017, 27, 1703198
[20] Tao T, Zhi T, Liu B, et al. Electron-beam-driven III-nitride plasmonic nanolasers in the deep-UV and visible region. Small, 2020, 16, 1906205
[21] Liu B, Smith R, Athanasiou M, et al. Temporally and spatially resolved photoluminescence investigation of ($11\bar{2}2$) semi-polar InGaN/GaN multiple quantum wells grown on nanorod templates. Appl Phys Lett, 2014, 105, 261103
[22] Liu B, Zhang R, Xie Z L, et al. Nonpolar m-plane thin film GaN and InGaN/GaN light-emitting diodes on $LiAlO_2$(100) substrates. Appl Phys Lett, 2007, 91, 253506

Ting Zhi received Ph.D. degree in solid state electronics from Nanjing University, Nanjing, China in 2016. She joined the College of Electronic and Optical Engineering & College of Microelectronics in Nanjing University of Posts and Telecommunications in 2016, where she is currently a lecturer of electrical science and engineering. Her interests include GaN based optical device, Micro-LED communication, PEC and plasmonic nanolaser devices.

Tao Tao received Ph.D. degree in solid state electronics from Nanjing University, Nanjing, China in 2015. He joined the school of electronic science and engineering in Nanjing University in 2015, where he is currently an associate professor of electrical science and engineering. His interests include growth of III-nitride semiconductors, micro-LED, nano-LED and plasmonic nanolaser devices.